

PAPER

# Optimal energy growth in a stably stratified shear flow

To cite this article: Sharath Jose *et al* 2018 *Fluid Dyn. Res.* **50** 011421

View the [article online](#) for updates and enhancements.

## You may also like

- [Optimal perturbations in viscous channel flow with crossflow](#)  
Cheng Chen, Jiang-Tao Huang and Wei-Guo Zhang
- [Investigation of the transient growth in plane jet by non-modal stability analysis](#)  
Siavash Gohardehi, Hossein Afshin and Bijan Farhanieh
- [Non-modal disturbances growth in a viscous mixing layer flow](#)  
H Vitoshkin and A Yu Gelfgat

# Optimal energy growth in a stably stratified shear flow

Sharath Jose<sup>1</sup>, Anubhab Roy<sup>2</sup>, Rahul Bale<sup>3</sup>,  
Krithika Iyer<sup>4</sup> and Rama Govindarajan<sup>5</sup>

<sup>1</sup> TIFR Centre for Interdisciplinary Sciences, Tata Institute of Fundamental Research,  
21 Brundavan Colony, Narsingi, Hyderabad 500075, India

<sup>2</sup> Department of Applied Mechanics, IIT Madras, Chennai 600036, India

<sup>3</sup> RIKEN-AICS, Kobe, Hyogo 6500047, Japan

<sup>4</sup> Mitsubishi Heavy Industries, Ritto, Shiga 5203080, Japan

<sup>5</sup> International Centre for Theoretical Sciences, Tata Institute of Fundamental Research,  
Bangalore 560089, India

E-mail: [rama@icts.res.in](mailto:rama@icts.res.in)

Received 30 December 2016, revised 1 May 2017

Accepted for publication 2 August 2017

Published 16 January 2018



CrossMark

Communicated by: Professor Jens Eggers

## Abstract

Transient growth of perturbations by a linear non-modal evolution is studied here in a stably stratified bounded Couette flow. The density stratification is linear. Classical inviscid stability theory states that a parallel shear flow is stable to exponentially growing disturbances if the Richardson number ( $Ri$ ) is greater than  $1/4$  everywhere in the flow. Experiments and numerical simulations at higher  $Ri$  show however that algebraically growing disturbances can lead to transient amplification. The complexity of a stably stratified shear flow stems from its ability to combine this transient amplification with propagating internal gravity waves (IGWs). The optimal perturbations associated with maximum energy amplification are numerically obtained at intermediate Reynolds numbers. It is shown that in this wall-bounded flow, the three-dimensional optimal perturbations are oblique, unlike in unstratified flow. A partitioning of energy into kinetic and potential helps in understanding the exchange of energies and how it modifies the transient growth. We show that the apportionment between potential and kinetic energy depends, in an interesting manner, on the Richardson number, and on time, as the transient growth proceeds from an optimal perturbation. The oft-quoted stabilizing role of stratification is also probed in the non-diffusive limit in the context of disturbance energy amplification.

Keywords: stratified flows, transient growth, internal gravity waves

(Some figures may appear in colour only in the online journal)

## 1. Introduction

Stable stratification, density increasing in the direction of gravity, is frequently observed in geophysical flows. Due to this density stratification, in both the atmosphere and the ocean, the medium allows for the propagation of internal gravity waves (IGWs) beyond a critical stratification. Stratified flows are often encountered in environments in the presence of shear flows and the interaction of stable stratification and mean shear offers a wide range of interesting physical phenomena (Turner 1973).

Stability of stratified shear flows, in both unbounded and bounded model geometries, have been studied well. For a uniformly stratified linear shear flow no exponential instabilities exist. Early studies focused on the long-time behavior of infinitesimal disturbances (see Jose *et al* (2015) and references therein). With increasing interest in transient stability of shear flows via a non-modal stability theory, an optimal energy growth based study of bounded and unbounded stratified Couette flow to two-dimensional disturbances was performed by Farrell and Ioannou (1993). Bakas *et al* (2001) used the optimal excitation technique to study the full three-dimensional viscous unbounded problem where the optimising time is a parameter to be specified. Consequently, upon increasing the optimising time, they found the corresponding optimal perturbations to be streamwise rolls. We will show below a different result in bounded Couette flow by systematically studying the variation of obliqueness with the Richardson number  $Ri$ . Biau and Bottaro (2004) and Sameen and Govindarajan (2007) (also see Sameen *et al* (2011)) studied Poiseuille flow and showed how stratification modifies transient growth. Again streamwise rolls are the ones that grow the most. A recent study (Jerome *et al* 2012) investigated the problem of stratified shear flow in both Couette and Poiseuille geometries, but in the context of a destabilizing temperature gradient. The present work is on a similar geometry as that of Jerome *et al* (2012), but our interest is in stable stratification and so the mechanism of disturbance growth is different. Recently Eaves and Caulfield (2015) studied initial conditions with the smallest possible perturbation energy density that can trigger turbulence from the laminar state of a stratified plane Couette flow using a nonlinear optimal perturbation analysis. They investigate the laminar-turbulent boundary or ‘edge’ and identify the nonlinear coherent states which are stratified analogues of the solutions described by Waleffe (1998). In section 4 we will comment on the findings of the present work in the context of the study of Eaves and Caulfield (2015).

In our recent study (Jose *et al* 2015) we analyzed the short-time evolution of disturbances in inviscid Couette flow via an initial value problem formulation by drawing an analogy with the popular lift-up effect, a dominant mechanism for the transient growth of three-dimensional disturbances in shear flows. Our analytical calculations showed how the perturbations in a uniformly stratified shear flow can grow algebraically in time due to buoyancy forces acting on the momentum variables. We demonstrated that perturbation energy can grow to large values even in two dimensions in the stratified case, unlike in constant density flow, where a three-dimensional nature of the disturbance is required. In the present study we will focus on the viscous problem and study optimal perturbations in a bounded stratified shear flow. It will be shown that unlike in most flow situations hitherto studied, where the optimal perturbation is streamwise invariant, the optimal perturbation here is one with a significant degree of obliqueness. Previously unexplored features of the optimal, such as the evolution of the ratio of kinetic to potential energy and obliqueness of the optimal mode, will be discussed.

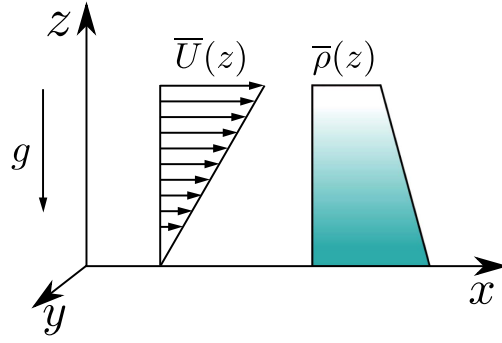


Figure 1. Flow schematic.

## 2. Problem formulation

### 2.1. Perturbation equations

We consider the stability of stratified fluid under the Boussinesq approximation (Spiegel and Veronis 1960). The mean state is composed of a shear flow,  $\bar{U}(z)$ , in an ambient density field,  $\bar{\rho}(z)$ , with gravity acting along the negative  $z$  direction (see figure 1).

For non-dimensionalization, we choose representative scales  $U_{ref}$  and  $L_{ref}$  for velocity and length respectively. On linearization about the mean, the stability equations describing the evolution of a three-dimensional velocity-density perturbation field can be written down as

$$\left[ \left( \frac{\partial}{\partial t} + \bar{U} \frac{\partial}{\partial x} \right) \nabla^2 - \bar{U}'' \frac{\partial}{\partial x} \right] w = -\text{Ri}_{ref} \nabla_H^2 \rho + \frac{1}{\text{Re}} \nabla^4 w, \quad (1)$$

$$\left( \frac{\partial}{\partial t} + \bar{U} \frac{\partial}{\partial x} \right) \eta = -\bar{U}' \frac{\partial w}{\partial y} + \frac{1}{\text{Re}} \nabla^2 \eta, \quad (2)$$

$$\left( \frac{\partial}{\partial t} + \bar{U} \frac{\partial}{\partial x} \right) \rho = \frac{N^2}{N_{ref}^2} w + \frac{1}{\text{Re Pr}} \nabla^2 \rho, \quad (3)$$

where  $w$  and  $\eta$  are the  $z$ -component of the velocity and vorticity perturbations respectively and  $\rho$  is the density perturbation.  $\nabla_H^2 = \frac{\partial^2}{\partial x^2} + \frac{\partial^2}{\partial y^2}$  is the horizontal Laplacian.  $N \equiv [-g\bar{\rho}'/\bar{\rho}_m]^{1/2}$  is the Brunt–Väisälä frequency, where  $\bar{\rho}_m$  is chosen as the mean value of background density, and  $N_{ref} \equiv \sqrt{g/L_{ref}}$  is a reference frequency.  $\text{Ri}_{ref} = (N_{ref} L_{ref} / U_{ref})^2 = g L_{ref} / U_{ref}^2$  is a reference Richardson number (or inverse squared Froude number  $\text{Fr}_{ref}^{-2}$ ) whereas it is the local Richardson number  $\text{Ri} = (N L_{ref} / U_{ref})^2$  which captures the local variation of density. The relative sizes of inertial to viscous and viscous to diffusive effects are represented respectively by the Reynolds number,  $\text{Re} = U_{ref} L_{ref} / \nu$  and the Prandtl number,  $\text{Pr} = \nu / \kappa$ . The kinematic viscosity of the fluid is  $\nu$ , while  $\kappa$  is its thermal/mass diffusivity.

An assumption of a normal mode form for the perturbation quantities as  $f(x, y, z, t) = \hat{f}(z, t) e^{ik_x x + ik_y y}$  will result in the following set of equations.

$$\frac{\partial \mathbf{q}}{\partial t} = \mathbf{A} \mathbf{q}. \quad (4)$$

$\mathbf{q} = [\hat{w} \ \hat{\eta} \ \hat{\rho}]^T$ , with appropriate boundary conditions as discussed below. Here,  $\mathbf{A} = \mathbf{M}^{-1} \mathbf{L}$ ,

$$\mathbf{M} = \begin{bmatrix} D^2 - k^2 & 0 & 0 \\ 0 & 1 & 0 \\ 0 & 0 & 1 \end{bmatrix},$$

$$\mathbf{L} = \begin{bmatrix} L_{OS} & 0 & k^2 \text{Ri}_{ref} \\ -ik_y \bar{U}' & L_{SQ1} & 0 \\ \frac{N^2}{N_{ref}^2} & 0 & L_{SQ2} \end{bmatrix},$$

$$L_{OS} = -ik_x \bar{U} (D^2 - k^2) + ik_x \bar{U}'' + \frac{1}{Re} (D^2 - k^2)^2,$$

$$L_{SQ1} = -ik_x \bar{U} + \frac{1}{Re} (D^2 - k^2),$$

$$\text{and } L_{SQ2} = -ik_x \bar{U} + \frac{1}{Re \text{ Pr}} (D^2 - k^2).$$

Above  $D = \partial/\partial z$  and  $k = \sqrt{k_x^2 + k_y^2}$ . The boundary conditions for the above equations are:  $\hat{w} = D\hat{w} = \hat{\eta} = \hat{\rho} = 0$  at  $z = \pm 1$ . For studying an inviscid, non-diffusive system, the conditions on  $D\hat{w}$  and  $\hat{\eta}$  are relaxed.

If the perturbation were to have an exponential dependence in time as well ( $\hat{f}(z, t) = \tilde{f}(z, t) e^{-ik_x c t}$ , with  $c$  being complex), we obtain the celebrated Taylor–Goldstein–Haurwitz equation for two dimensional disturbances ( $k_y = 0$ ) when viscous and diffusion effects are neglected (Drazin and Reid 1981):

$$(\bar{U} - c)[(\bar{U} - c)(D_*^2 - k_x^2) - \bar{U}'] \tilde{w} + \text{Ri} \tilde{w} = 0, \quad (5)$$

with  $D_* = d/dz$ . On incorporating viscous and diffusive dynamics we get,

$$[(D_*^2 - k_x^2) - ik_x \text{RePr}(\bar{U} - c)][(D_*^2 - k_x^2)^2 - ik_x \text{Re}\{(\bar{U} - c)(D_*^2 - k_x^2) - \bar{U}''\}] \tilde{w} \\ = k_x^2 \text{Pr} \text{Re}^2 \text{Ri} \tilde{w}. \quad (6)$$

Classical linear stability entails solving one of the above equations for given boundary conditions as an eigenvalue problem. It is a well-known fact that the Taylor–Goldstein–Haurwitz equation (5) is a singular equation in the same way as its constant density counterpart—the Rayleigh equation. If we now include a non-zero viscosity, but allow the Prandtl number to tend to infinity, we are left with a less severe form of the singularity. While velocity and vorticity are regular at the location of singularity (Engevik 1974, Koppel 1964), density is conserved along streamlines, so equation (6) with  $\text{Pr} \rightarrow \infty$  allows the density to maintain arbitrarily large cross-stream gradients.

## 2.2. Optimal perturbation analysis

The optimal perturbations can be obtained by extremizing an objective functional, chosen based on the physical quantity of interest. As often is done in hydrodynamic stability, we choose the disturbance energy as the desired objective functional. Though beyond the scope of the present analysis, we remark that for stratified flows the desired object to be extremized

could be a quantity different from the energy, for example, an objective functional could be a measure of mixing. Foures *et al* (2014) has recently carried out nonlinear optimisation of a passive scalar mixing in plane Poiseuille flow based on a mixing norm defined by Mathew *et al* (2005). Future studies investigating the optimisation of mixing norms in buoyancy driven flows, relevant for stratified shear flows, would be very useful.

The objective functional to be maximized here is the total energy normalized by its initial value, commonly known as the gain:

$$G = \frac{E(k_x, k_y; t)}{E(k_x, k_y; 0)}. \quad (7)$$

$E$  gives the total energy of the perturbation with both kinetic and potential contributions (Kaminski *et al* 2014), and is of the following form.

$$E = \frac{1}{8k^2} \int_{-1}^1 (k^2 w^* w + D w^* D w + \eta^* \eta + \text{Ri} k^2 \rho^* \rho) dz. \quad (8)$$

For a given wavenumber vector, the approach to find the optimal involves scanning the space of all initial conditions and finding the one which provides us with the maximum energy amplification. The global optimal perturbation is the initial condition that leads to the largest gain  $G_{\max}$ , optimised over all possible wavenumbers and time. The corresponding wavenumber pair and the time at which the maximum energy amplification are consequently labelled as optimal quantities.

The search for the optimal perturbation can be done using two popular techniques—the singular value decomposition (SVD) technique (Schmid and Henningson 2001) and the power iteration technique (Corbett and Bottaro 2000). Both methods involve solving the discretised version of the linearised system of equations. In the linear case, the power iteration technique is particularly useful when one deals with unbounded systems. Unbounded shear flows contain viscous continuous spectra (Grosch and Salwen 1978) and SVD, which involves expanding over a finite basis of eigenfunctions, may underestimate the energy amplification by not appropriately capturing the contribution from the viscous continuous spectrum (Guégan *et al* 2006). However, for bounded systems such as the one being studied here, SVD is more suited than power iteration due to its computational efficiency. We have performed calculations using both techniques and cross-validated our numerics, but the results presented have been obtained using an SVD analysis.

### 3. Results

Plane Couette flow is exponentially stable to infinitesimal disturbances for all Reynolds numbers (Romanov 1973). Given the large number of parameters in the problem, it is only feasible to explore a restricted region in parameter space. We fix the Reynolds number to be 500. The inclusion of bottom heavy linear density stratification leads to further stabilization and for higher stratification introduces IGWs (for  $\text{Ri} > 1/4$  in the inviscid case). Incidentally, even if density is ‘stably’ stratified, exponential instabilities can result if the Brunt–Väisälä frequency  $N$  is non-uniform (Taylor 1931, Huppert 1973). For our purposes, a linear stratification (constant  $N$ ) is sufficient, and the reference frequency  $N_{\text{ref}}$  is chosen to be equal to the Brunt–Väisälä frequency  $N$ . This implies  $\text{Ri} = \text{Ri}_{\text{ref}}$ , with a density difference  $\Delta \rho = 2 \bar{\rho}_m$  specified across the channel.

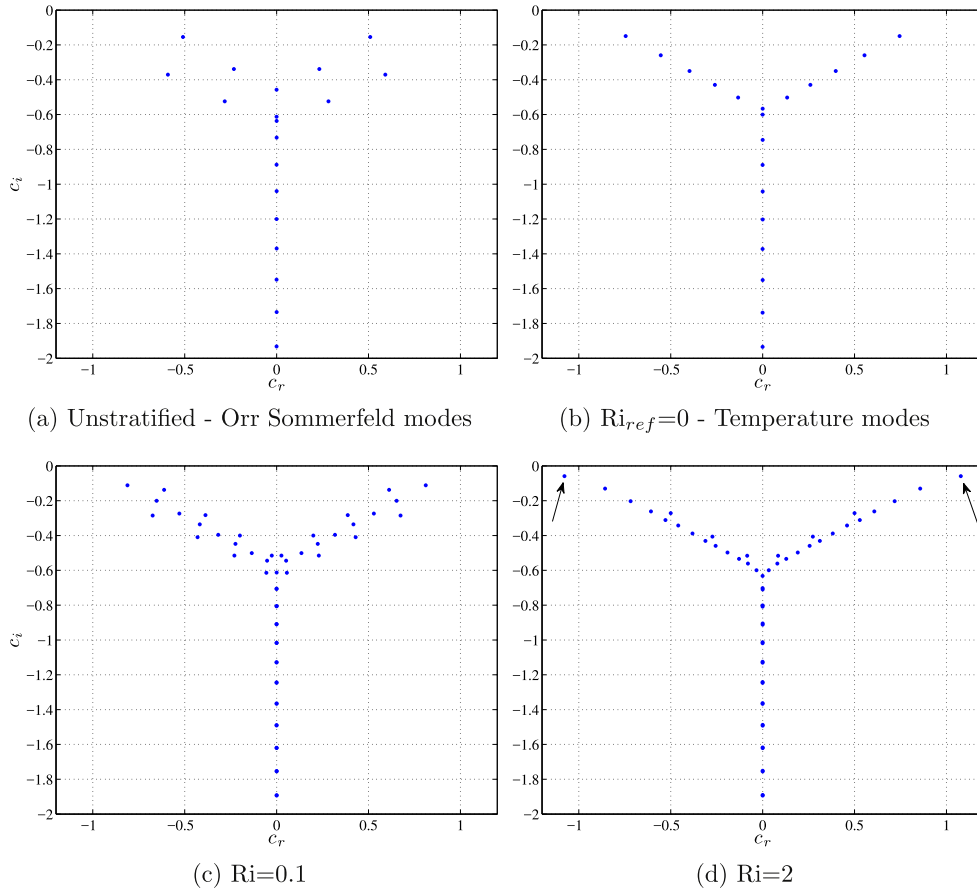


**Figure 2.** Spectrum for two-dimensional stability of viscous stratified Couette flow.  $Re = 500$ ,  $Pr = 1$ . Arrows in (d) indicate damped IGWs.

### 3.1. Spectrum of the linearised operator

We first briefly discuss the spectrum of the linearised operator. The two-dimensional viscous spectrum for stratified Couette flow can be seen in figure 2. To maintain clarity only modes with  $c_i > -2$  are shown. The familiar Orr-Sommerfeld (OS) spectrum can be seen in figure 2(a). To display temperature modes (Davey and Reid 1977) alone, we set  $Ri_{ref} = 0$ , in figure 2(b). Due to the similarity between equations (3) and (2), the temperature spectrum is very close to the Squire spectrum of the three-dimensional homogeneous problem. Based on this it would seem possible that a resonance mechanism exists between the OS and temperature modes, similar to the one between OS and Squire modes (Gustavsson and Hultgren 1980). As known from Gustavsson and Hultgren (1980) for the constant density case, such resonance mechanism could be specific to certain wave-numbers and may be swamped by more global non-modal growth physics, e.g. the Orr mechanism or the lift-up effect. For weak stratification (figure 2(c)) the spectrum is a combination of the OS and temperature modes. With increasing stratification the spectrum gets more complicated and viscously damped IGWs appear, as indicated by arrows in figure 2(d).

For three-dimensional perturbations, it is interesting to note that stratification leaves the Squire spectrum unaltered, and this has important consequence for the transient growth exhibited by the system. From a modal perspective we know that the transient amplification of three-dimensional disturbances in shear flows occur due to the de-phasing of OS and Squire modes, which at  $t = 0$  constituted an initial condition devoid of normal vorticity (Schmid and Henningson 2001). We anticipate thus that the lift-up effect will continue to be the most dominant non-modal growth physics even with the inclusion of stratification.

Having discussed the modal characteristics of stratified Couette flow, we next focus on non-modal physics. This would be studied via finding the optimal perturbations.

### 3.2. Two-dimensional optimal perturbations

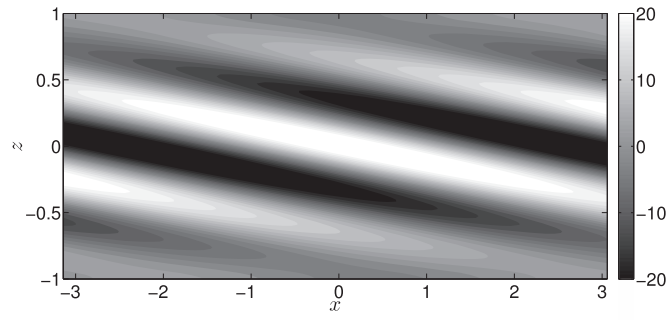
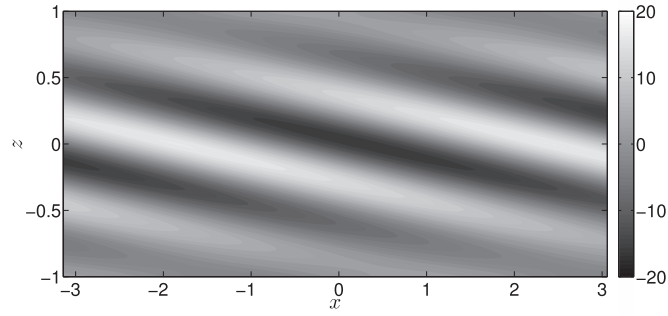
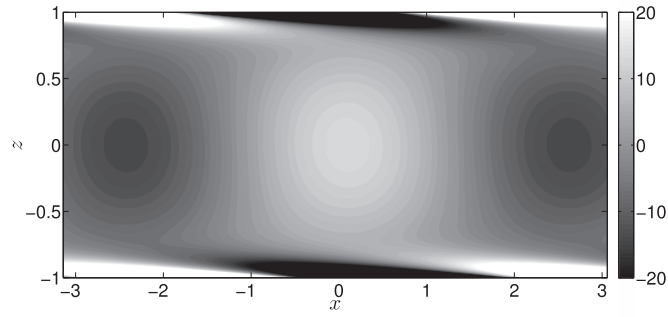
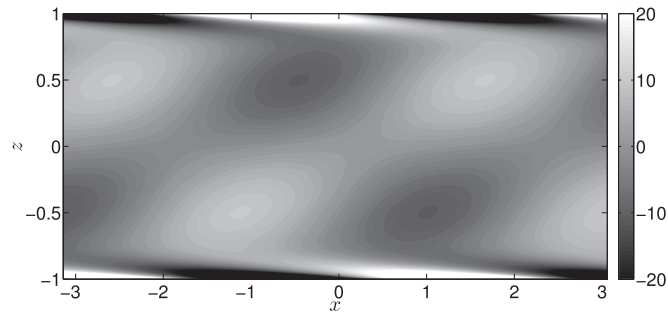
With the introduction of viscosity, our system is stable in the linear sense, in that all eigenfunctions decay exponentially. The optimal initial perturbation yields the highest possible growth of total energy, i.e.  $G_{\max}$  at a time  $T_{\text{opt}}$ , beyond which time there is a decay in perturbation energy. The termination of this growth occurs due to the diffusion of the localized density perturbation, which depends on the Péclet number ( $\text{Pe} = \text{Pr Re}$ ), and diffusion of momentum given by  $\text{Re}$ .

For two-dimensional flows with stream-wise variation of disturbances, viscosity cuts off disturbance growth on a time scale of  $O(\text{Re}^{1/3})$  (Moffatt 1967). In our earlier work (Jose *et al* 2015), with background stratification specified to be strong as in the present case, we find disturbance energy growing as  $t^{2n+1}$  ( $n = \sqrt{0.25 - \text{Ri}}$ ) before decaying as  $t^{-3+2n}$  at later times. Thus sub-linear growth, if present, would lead to an amplification of at most  $O(\text{Re}^{(2n+1)/3})$  which for any non-zero  $\text{Ri}$  would be less than the  $O(\text{Re}^{2/3})$  amplification observed due to Orr mechanism.

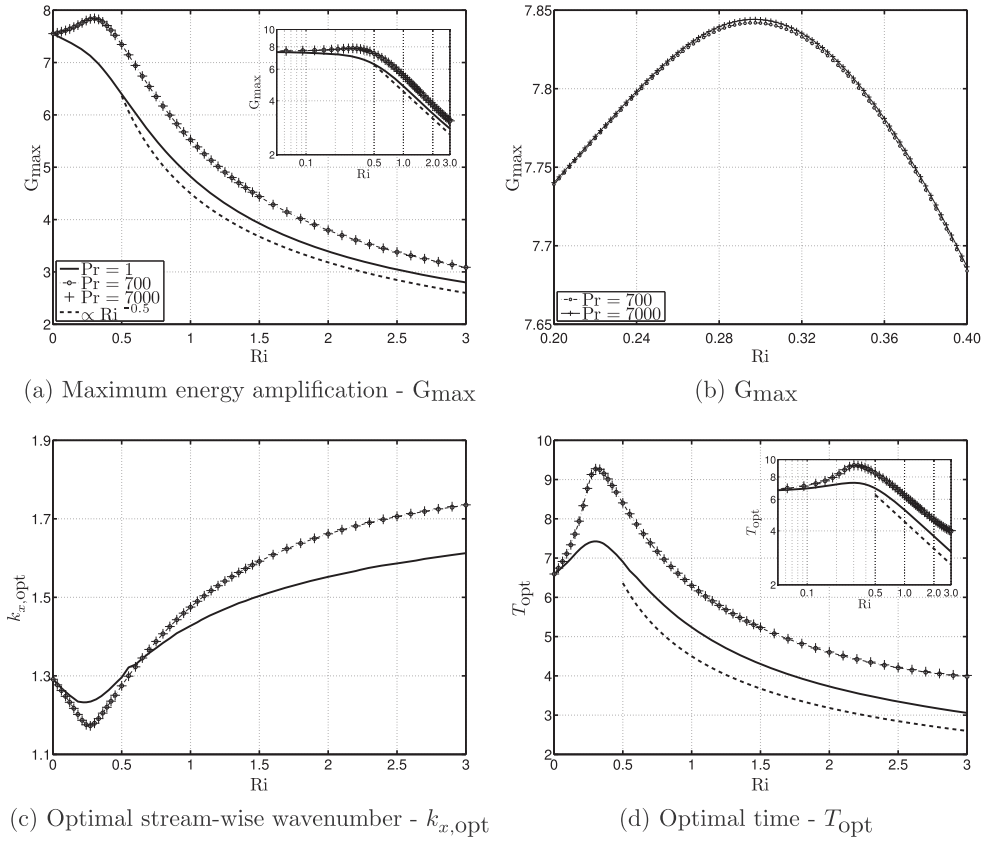
At the Reynolds number at which we present our results (500), the Orr-mechanism, which gives the highest energy growth in an unstratified system, thus dominates as the optimal perturbations even in presence of stratification. This is evident from figure 3, where optimal vorticity perturbations at  $t = 0$  and their evolved structure at  $t = T_{\text{opt}}$  are shown. Since stratification is unimportant for this mechanism, the behavior is similar whether stratification is weak,  $\text{Ri} = 0.1$ , or strong,  $\text{Ri} = 1$ . The initial condition consists of upstream leaning structures, which are progressively straightened by the background shear. As is known in the unstratified case, up to the point where the structures become vertical, the Reynolds stresses aid in energy transfer from the mean flow to the perturbations, and so we obtain energy growth up to this time. The optimal density perturbations mimics the optimal vorticity perturbations with its up-shear tilt.

Figure 4 shows the variation of  $G_{\max}$ , the streamwise wavenumber  $k_{x,\text{opt}}$  of the optimal perturbation, and the optimal time  $T_{\text{opt}}$ , with stratification ( $\text{Ri}$ ). At this Reynolds number, we have seen that the dominant reason for energy amplification in two-dimensions is the Orr mechanism. Stratification resists vertical motion, which translates into the inhibition of energy amplification by the Orr mechanism. This is easily seen for  $\text{Pr} = 1$  in figure 4(a). But interestingly poor diffusivity of the density field ( $\text{Pr} \gg 1$ ) leads to a higher amplification, which for weak stratification (small  $\text{Ri}$ ) can result in more energy growth than the unstratified case (figures 4(a) and (b)). The contributions to  $G_{\max}$  come from both kinetic and potential energies. With increasing stratification, buoyancy affords increasing resistance to vertical motion, corresponding to lower perturbation kinetic energy and higher potential energy. Lowered diffusivity of the density field,  $\text{Pr} \gg 1$ , leads to further preservation of potential energy. The combination of the two allows for  $G_{\max}$  exhibiting a peak at non-zero  $\text{Ri}$  for  $\text{Pr} \gg 1$ .



(a)  $Ri=0.1$ ,  $Pr=700$ ,  $t = 0$ (b)  $Ri=1$ ,  $Pr=700$ ,  $t = 0$ (c)  $Ri=0.1$ ,  $Pr=700$ ,  $t = T_{\text{opt}}$ (d)  $Ri=1$ ,  $Pr=700$ ,  $t = T_{\text{opt}}$ 

**Figure 3.** Optimal perturbations in the  $x - z$  plane for  $Ri = 0.1$  and  $1$  at  $t = 0$  and  $t = T_{\text{opt}}$ . Shown here are isocontours of spanwise perturbation vorticity.



**Figure 4.** Dependence of optimal  $G_{\max}$ ,  $k_{x,opt}$  and  $T_{opt}$  on stratification ( $Ri$ ) for various values of  $Pr$ . (b) is a zoomed-in version of (a) highlighting the marginally larger values for  $Pr = 7000$  over that of  $Pr = 700$ .

In an inviscid study based on convected plane-waves (Farrell and Ioannou 1993), a WKB analysis for large  $Ri$  reveals

$$\frac{E(t)}{E(0)} = \sqrt{\frac{E_0(t)}{E_0(0)}} \quad (9)$$

where  $E$  and  $E_0$  respectively are the total energy for highly stratified ( $Ri \gg 1$ ) and unstratified ( $Ri = 0$ ) flows. Figure 4(a) offers, in the viscous case, a signature for this asymptotic behaviour, where  $G_{\max, Ri \gg 1} \sim \sqrt{G_{\max, Ri=0}}$ . For the unstratified case, at  $Re = 500$ , the optimal growth obtained for two-dimensional disturbances is 7.55; the corresponding optimal streamwise wavenumber and optimal time are 1.29 and 6.58 respectively. At higher  $Ri$ , we see that the values of  $G_{\max}$  start approaching those as predicted by the WKB analysis of Farrell and Ioannou (1993).

Both  $k_{x,opt}$  and  $T_{opt}$  (figures 4(c)–(d)) show a clear demarcation of dynamics on either side of  $Ri \approx 0.25$ . For a uniformly stratified Couette flow, according to inviscid theory,  $Ri = 0.25$  indicates the onset of sheared IGWs. At any  $Ri$  greater than this value, the dynamics is largely influenced by IGWs. That this is true in viscous flow as well is visible in figure 4(d) where the  $T_{opt}$  scales with  $Ri^{-0.5}$ , and is thus just a measure of the inverse of  $N$ , the Brunt–Väisälä

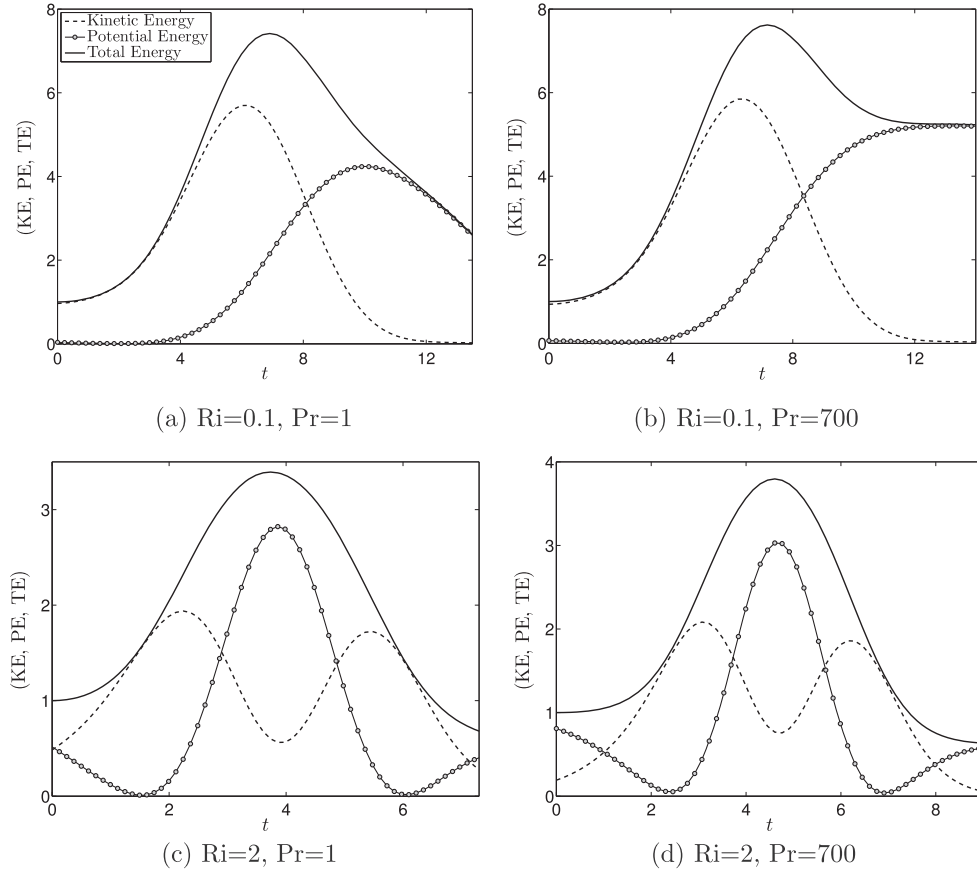


**Figure 5.** Temporal evolution of perturbation kinetic, potential and total energy for various two levels of stratification and two levels of diffusivity, for an excitation corresponding to the optimal initial condition.

frequency. At high  $Ri$  the algebraic growth dynamics is thus dominated by IGWs instead of background shear.

An important feature in the context of stratified shear flows that is often overlooked in optimal perturbation calculations is the ‘energy partitioning’; i.e. the ratio of potential energy (PE) to kinetic energy (KE). In figure 5 the temporal evolution of the total energy and its two components is shown for optimal initial condition excitations for high and low  $Ri$ , and high and low mass diffusivity. When  $Ri$  is low, the momentum forcing describes the total energy evolution almost till the optimal time, beyond which the buoyancy component sustains it. At high values of  $Ri$ , IGWs set in and the energy evolution is contributed to by both momentum and buoyancy forcing. The maximum energy amplification occurs at the maximum of PE. As one can intuitively imagine, with increasing stratification, the initial forcing will transition from a purely momentum one to an increasingly buoyant one (figure 6(a)). But at the optimal instant this ratio saturates with increasing stratification (figure 6(b)).

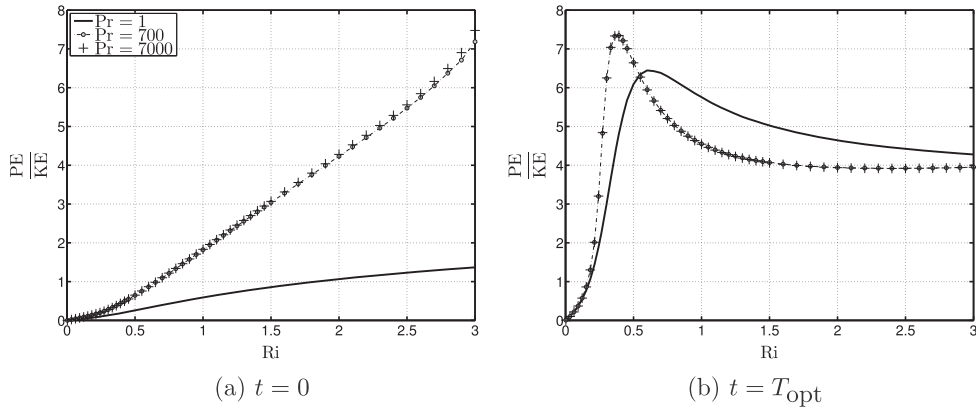


**Figure 6.** Dependence of the ‘energy partitioning’ ratio ( $PE/KE$ ) on stratification ( $Ri$ ) at the initial instant (a) and optimal time (b).

### 3.3. Three-dimensional optimal perturbations

For three-dimensional disturbances in unstratified shear flows, the dominant transient growth mechanism is the ‘lift-up’ effect that entails redistribution of momentum by fluid parcels traveling vertically. In the homogeneous problem the optimal initial condition is that of a stream-wise aligned ‘roll’ – a span-wise varying normal velocity field. These rolls stay streamwise aligned during the energy growth phase and beyond. In contrast, figure 7 depicts the evolution of the optimal velocity perturbation in the presence of stratification. With the inclusion of stratification the optimal ‘rolls’ turn oblique. This obliqueness, or stream-wise dependence, also introduces an up-shear tilt in the flow-gradient plane ( $x$ – $z$ ) thus demonstrating that the Orr mechanism is acting in unison with the more dominant lift-up effect. The optimal structure thus evolves in time, changing both its obliqueness and its shape. This high obliqueness and its evolution of the optimal perturbation is an interesting feature of bounded viscous stratified flow, not obtained up to now, to our knowledge.

The lift-up effect is reliant on the vertical motion of fluid parcels, riding along the background shear, dynamics which stable stratification must resist. Thus stable stratification, in three dimensions as well, reduces transient amplification, as seen in figure 8. It is notable how drastically the maximum amplification achieved falls with increasing stratification. At  $Ri \sim O(1)$ , the values of  $G_{max}$  obtained for two and three dimensional disturbances are nearly equal. The effect of stratification in strongly suppressing transient amplification is thus apparent. Unlike in unstratified flows, at high  $Ri$ , there would not be significant differences in the levels of  $G_{max}$  for streamwise independent and spanwise independent disturbances. Our analysis for spanwise independent disturbances appears to be consistent with the large  $Ri$  asymptote for energy amplification as derived by Farrell and Ioannou (1993). This indicates the possibility that  $G_{max}$  will not be affected at high  $Ri$  due to increasing obliqueness ( $k_{y,opt} \rightarrow 0$ ) of the optimal initial perturbation.

There is a contrast with two-dimensional results, in that there is no change of behaviour at around  $Ri=0.25$ , may seem surprising at first. However, this is resolved when we remember that the low  $Ri$  response is dictated by the ‘lift-up’ effect, so  $k_{x,opt} \rightarrow 0$  as  $Ri \rightarrow 0$ . For small  $Ri$ , with vanishing streamwise dependence, the vertical velocity and buoyancy equation can be reduced from (4)–(5) to

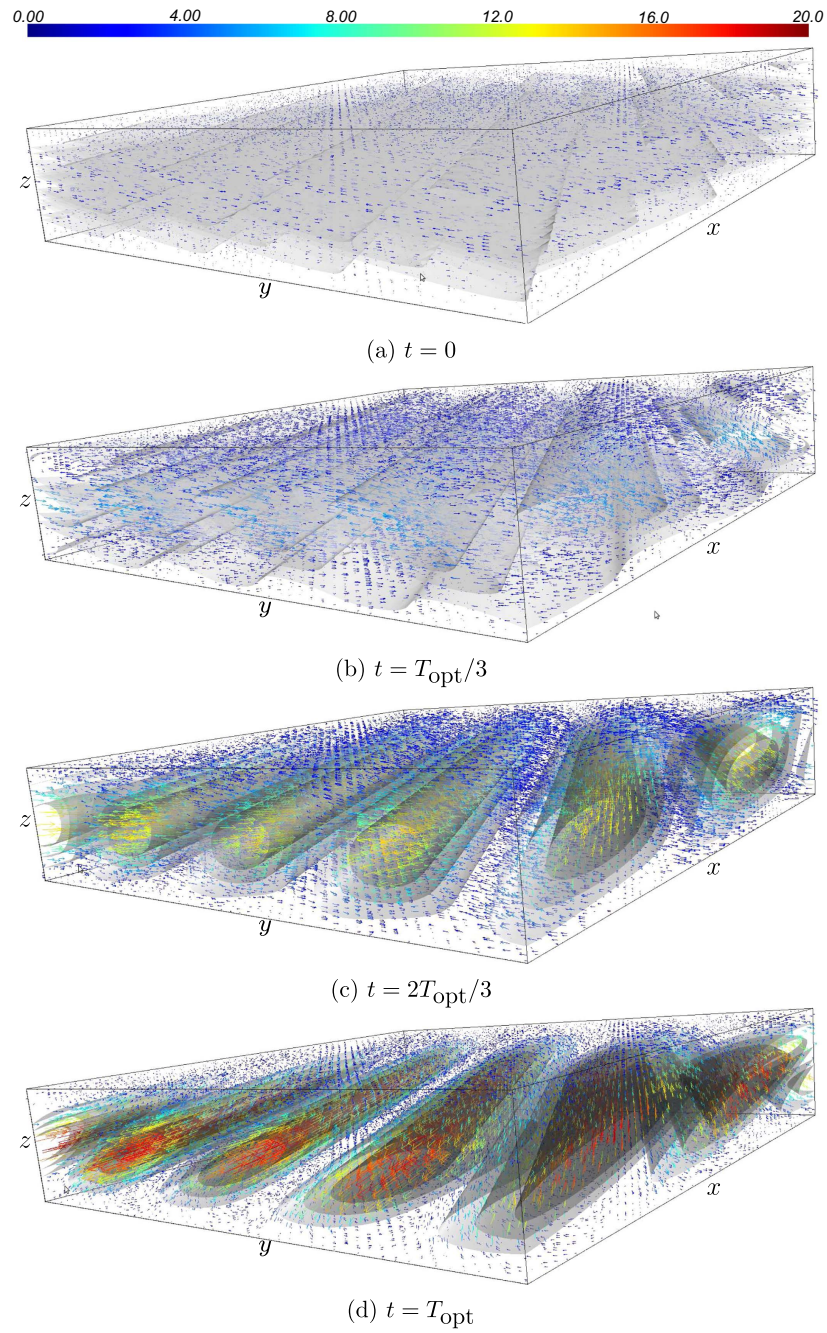


**Figure 7.** Evolution of optimal perturbation velocity.  $\text{Re} = 500$ ,  $\text{Ri} = 0.1$ ,  $\text{Pr} = 1$ .

$$\frac{\partial}{\partial t}(\mathbf{D}^2 - k_y^2)w = k_y^2 \text{Ri}_{\text{ref}} \rho \quad (10)$$

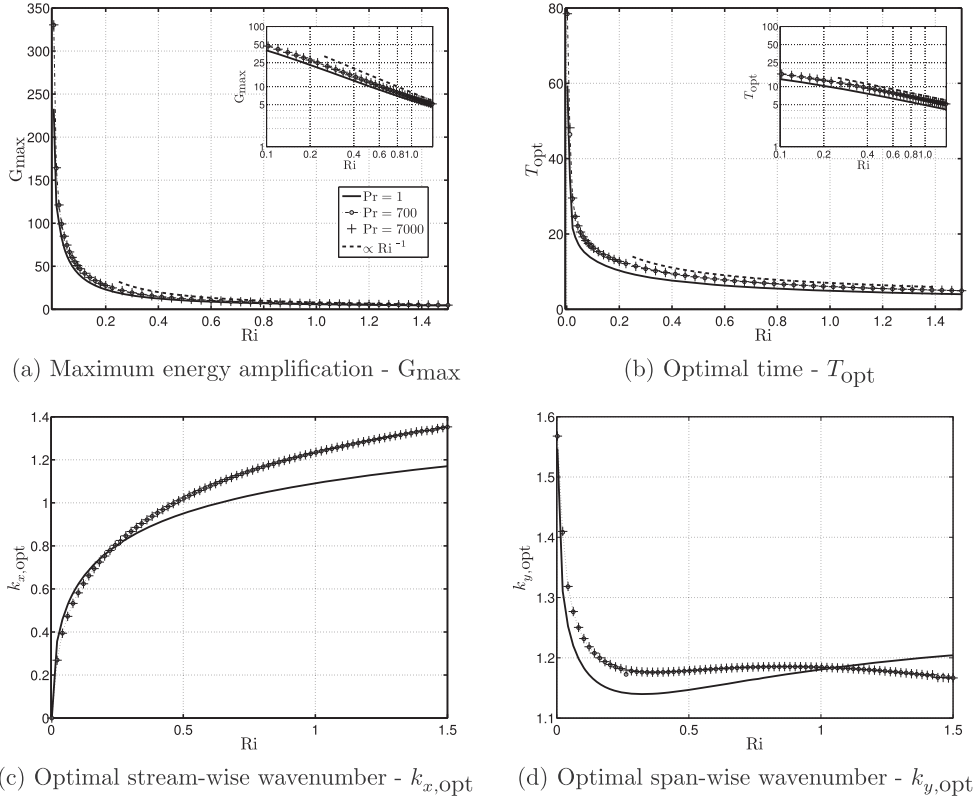


**Figure 8.** Dependence of optimal  $G_{\max}$ ,  $k_{x,\text{opt}}$ ,  $k_{y,\text{opt}}$  and  $T_{\text{opt}}$  on stratification ( $Ri$ ) for various values of  $Pr$ .

$$\frac{\partial}{\partial t} \rho = \frac{N^2}{N_{\text{ref}}^2} w, \quad (11)$$

which can be combined into a single equation in which shear plays no role:

$$\frac{\partial^2}{\partial t^2} (D^2 - k_y^2) w = k_y^2 Ri w. \quad (12)$$

The above system supports IGWs for any non-zero  $Ri$ . The oscillating vertical velocity field forces the normal vorticity equation. The optimal time  $T_{\text{opt}}$  scales with the buoyancy time scale ( $\sim Ri^{-0.5}$ ), as seen in figure 8(d)). The amplification, which depends on the optimal time as  $T_{\text{opt}}^2$ , scales as  $O(Ri^{-1})$  (figure 8(a)). Bakas *et al* (2001) too predict the same scaling for unbounded stratified Couette flow.

In this flow where stratification introduces an obliqueness, it is instructive to quantify the effect of stratification on the obliqueness of the optimal initial condition. The obliqueness is measured as

$$\theta = \tan^{-1} \left[ \frac{k_{y,\text{opt}}}{k_{x,\text{opt}}} \right], \quad (13)$$

so  $\theta = \pi/2$  corresponds to a streamwise independent structure, with  $k_{x,\text{opt}} = 0$ . In an unstratified Couette flow,  $k_{x,\text{opt}} = 35/Re$ , so the optimal initial condition is practically

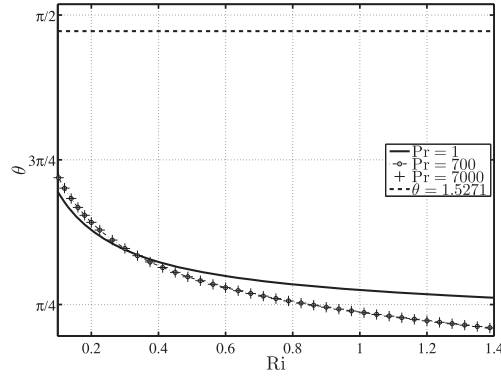


**Figure 9.** Variation of obliqueness of the optimal perturbation with stratification.  $\theta = 1.5271$ , for  $k_{x,opt} = 35/Re$  and  $k_y = 1.6$ , is the optimal obliqueness for unstratified Couette flow.  $\theta = \pi/2$  refers to streamwise independent structures.

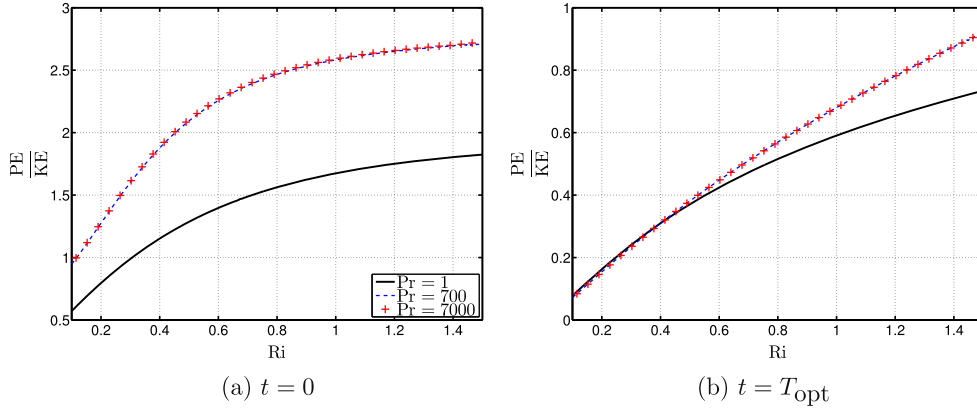


**Figure 10.** Variation of 'energy partitioning' (PE/KE) with stratification (Ri) at the initial instant (a) and optimal time (b).

streamwise independent at high Reynolds numbers. With increasing stratification, the initial condition becomes increasingly oblique, see figure 9, so the competing influence of the Orr mechanism is evident.

In figure 10, we show the ratio PE/KE for the three-dimensional optimal perturbations at the initial and the optimal times. Unlike an two-dimensional perturbations, in three-dimensions the flow field at  $t = T_{opt}$  is momentum dominated for the range of Ri that has been considered. It should be noted that the range of Ri accessed in the three-dimensional analysis here is smaller than that employed for the two-dimensional analysis. The apparent rise in PE/KE with Ri should also be seen in light of the fact that the background stratification increasingly inhibits vertical fluid motion.



## 4. Conclusions

We have examined in some detail how optimal perturbations in both two and three dimensions depend on the stratification. For the Reynolds number studied, the Orr mechanism is dominant in two dimensions, with added physics brought about by the potential energy of the perturbations and the possibility of one kind of energy converting to another. In three dimensions, there is an interplay between the Orr and the lift-up mechanisms, to create highly oblique optimal perturbations, rather than the streamwise independent structures in an unstratified flow. The obliqueness increases with stratification. Moreover, the optimal structure evolves in both shape and orientation, from the initial instant to the optimal time and beyond. At higher levels of stratification, the optimal growth  $G_{\max}$  and the optimal time  $T_{\text{opt}}$  are shown to obey scalings defined on bulk Richardson number  $Ri$ .

Eaves and Caulfield (2015) in their nonlinear optimal perturbation analysis observe that the well-known unstratified coherent states are disrupted due to stratification. The streamwise independent streaks that occur for  $Ri=0$  are no longer sustained when stratification is introduced. Due to the difference in objective, linear analysis maximizes the energy gain of disturbances while the nonlinear analysis seeks the turbulence triggering disturbance with the least energy, optimal perturbations of the linearized stability operator are not necessarily an approximation for the finite amplitude optimals (Pringle and Kerswell 2010). In the unstratified case, the linear optimal is 2D (streamwise independent rolls) while the nonlinear optimal is 3D. In the present work the optimals found are highly three-dimensional and we have both the Orr mechanism as well as the lift-up effect acting in unison initially, and with increasing stratification the flow deviates from streamwise independent streaks at  $t = T_{\text{opt}}$  as highlighted in great detail by Eaves and Caulfield (2015). We observe strong obliqueness in the initial condition with increasing  $Ri$  and the perturbation energy evolves in an oscillatory fashion. For the largest  $Ri$  accessed by Eaves and Caulfield (2015) ( $Ri = 10^{-2}$ ), they observe that the flow transitions to a chaotic state with a weak oscillation. We believe the present work can serve as a useful template for future nonlinear optimal perturbation analysis of flow regimes that are strongly dominated by IGWs. It would also be interesting to observe the role of nonlinearity on the partitioning of perturbation energy.

## Acknowledgments

We would like to dedicate this paper to Professor Keith Moffatt, who is, to our knowledge, the first person who demonstrated the algebraic growth of three-dimensional disturbances in a shear flow via a linear, inviscid interaction of the mean shear with longitudinal vortices. This later led to a whole field of study, including our work. RG thanks funding from the Ocean Mixing and Monsoon project of the the Ministry of Earth Sciences.

## References

- Bakas N, Ioannou P and Kefaliakos G 2001 *J. Atmos. Sci.* **58** 2790–806
- Biau D and Bottaro A 2004 *Phys. Fluids* **16** 4742–5
- Corbett P and Bottaro A 2000 *Phys. Fluids* **12** 120–30
- Davey A and Reid W H 1977 *J. Fluid Mech.* **80** 509–25
- Drazin P and Reid W 1981 *Hydrodynamic Stability* (Cambridge: Cambridge University Press)
- Eaves T and Caulfield C 2015 *J. Fluid Mech.* **784** 548–64
- Engvik L 1974 *Acta Mech.* **19** 169–78
- Farrell B and Ioannou P J 1993 *J. Atmos. Sci.* **50** 2201–14



- Foures D, Caulfield C and Schmid P J 2014 *J. Fluid Mech.* **748** 241–77
- Grosch C and Salwen H 1978 *J. Fluid Mech.* **87** 33–54
- Guégan A, Schmid P J and Huerre P 2006 *J. Fluid Mech.* **566** 11–45
- Gustavsson L H and Hultgren L S 1980 *J. Fluid Mech.* **98** 149–59
- Huppert H 1973 *J. Fluid Mech.* **57** 361–8
- Jerome J S, Chomaz J M and Huerre P 2012 *Phys. Fluids* **24** 044103
- Jose S, Roy A, Bale R and Govindarajan R 2015 *Proc. R. Soc. A* **471** 20150267
- Kaminski A K, C P Caulfield C and Taylor J R 2014 *J. Fluid Mech.* **758** R4
- Koppel D 1964 *J. Math. Phys.* **5** 963–82
- Mathew G, Mezić I and Petzold L 2005 *Physica D* **211** 23–46
- Moffatt H K 1967 *Atmospheric Turbulence and Radio Wave Propagation* ed A M Yaglom and V I Tatarsky (Moscow: Nauka) pp 139–54
- Pringle C C T and Kerswell R R 2010 *Phys. Rev. Letters* **105** 154502
- Romanov V A 1973 *Functional Anal. & Its Applics* **7** 137–46
- Sameen A, Bale R and Govindarajan R 2011 *J. Fluid Mech.* **673** 603–5
- Sameen A and Govindarajan R 2007 *J. Fluid Mech.* **577** 417–42
- Schmid P and Henningson D 2001 *Stability and Transition in Fluid Flows* (New York: Springer)
- Spiegel E and Veronis G 1960 *Astrophys. J.* **131** 441–7
- Taylor G 1931 *Proc. Roy. Soc. A* **132** 499–523
- Turner J 1973 *Buoyancy Effects in Fluids* (Cambridge: Cambridge University Press)
- Waleffe F 1998 *Phys. Rev. Letters* **81** 4140